Journal of Applied Polymer Science

Improvement of Adhesion and Continuity of Polypyrrole Thin Films Through Surface Modification of Hydrophobic Substrates

Namita Dutta Gupta,[1] Swati Das,[1] Nirmalya Sankar Das,[2] Diptonil Banerjee,[2] Debabrata Sarkar,[1] Kalyan Kumar Chattopadhyay[1,2]

[1]Thin Films and Nanoscience Laboratory, Department of Physics, Jadavpur University, Kolkata 700032, India
[2]School of Material Science and Nanotechnology, Jadavpur University, Kolkata 700032, India
Correspondence to: K. K. Chattopadhyay (E-mail: kalyan_chattopadhyay@yahoo.com)

ABSTRACT: Conducting polymer polypyrrole is reported to have a poor adhesion to substrate which limits its applicability as thin films. In this article, we report synthesis of well-formed and continuous film of polypyrrole through treatment of hydrophobic substrates. However, in place of the widely used organosilanes, the substrates were simply treated with surfactant cetyl trimethylammonium bromide (CTAB) prior to vapor phase polymerization under controlled environment. Polypyrrole films formed on CTAB pretreated substrates were found to have improved adhesion and continuity compared to the films formed on untreated substrates. The improved adhesion results in better electronic properties as seen during Electron field emission studies. Based on contact angle analysis, we propose that CTAB molecules act as anchoring agents for the oxidant layer on the substrate and hence assist in the deposition of a more continuous polypyrrole film. © 2013 Wiley Periodicals, Inc. J. Appl. Polym. Sci. Appl. Polym. Sci. **2014**, *131*, 39771.

KEYWORDS: coatings; conducting polymers; surfactants

Received 9 April 2013; accepted 15 July 2013
DOI: 10.1002/app.39771

INTRODUCTION

Conducting polymers such as polypyrrole (PPy) have been extensively studied for their unique physical and chemical properties and hence diverse application in various fields such as organic electronic devices,[1] chemical and biological sensors,[2] and electromagnetic shielding applications.[3] For novel device applications, it is desirable to synthesize PPy as thin films, on flexible hydrophobic substrates like PET (Polyethylene terephthalate), polyester, and other different fabrics. Thin films of PPy are usually prepared by chemical process (and a subsequent process such as spin coating) or by electrochemical method, both the methods being in liquid phase.[4–6] In addition to these two processes, a new method of polymerization of pyrrole monomers on the substrate surface, directly from vapor phase has also been recently reported.[7–10] This technique has a lot of advantages over the other method of deposition of PPy. For example, in liquid phase, the presence of a transport medium increases the probability of particle agglomeration. In vapor phase, however, such probability does not exist and hence the use of dispersants or stabilizers is not necessary. Moreover, in vapor phase, polymerization can occur in different types of substrates in contrast to electrochemical method, where only conducting substrates can be used.

One of the major obstacles for PPy film formation is the poor adhesion of PPy molecules to the substrate surface.[11] Though polymerization of pyrrole does not depend on the substrate, the polarity of the substrates has an important bearing on the adhesion of the polymer. The adhesion is worse for substrates without polar groups.[12] In order to overcome the problem of adhesion, the substrate surface is usually pretreated with an adhesive promoter layer, such as different types of organosilanes[13,14] or polymer (PVA and PFO) containing oxidants[10,15,16] before exposing to pyrrole vapors. These adhesion promoter molecules are appropriately functionalized organic molecules which allow anchoring of the polymer molecules on the substrate surface. For example, the adhesion promoter molecules like 3-((pyrrol-1yl) propyl trimethoxysilane,[17,18] 6-(pyrrol-1-yl)-*n*-hexyl trichlorosilane,[19] and other pyrrole substituted organosilane monolayers[20,21] consist of an adhesive group to the substrate, an alkyl spacer, and a terminal pyrrole group,[22] the last acting as nucleation sites of PPy films with good adhesion. Many authors have also proposed plasma treatment of the substrates as an alternative to increase the adhesion between the substrate and conducting polymer.[23–25] Plasma modification is reported to increase the wettability of the substrate due to increase of their surface energy.

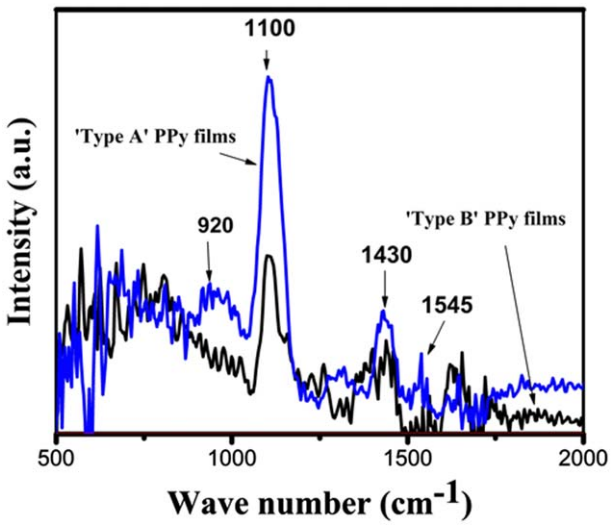

Figure 1. FTIR absorption spectra of PPy films of Type A and B deposited from vapor phase deposition technique. [Color figure can be viewed in the online issue, which is available at wileyonlinelibrary.com.]

In this article, instead of the conventional adhesion promoter material or plasma treatment, we have adopted a new technique of surface treatment of the hydrophobic substrates for formation a uniform and continuous PPy film, by simply treating the substrates with surfactants, prior to polymerization. Surfactants, like Cetyl trimethylammonium bromide, are mostly used in the synthesis of nanostructured polymers through micellar nucleation method.[26–28] Here a new role of surfactants as anchoring agents, for the formation of a uniform and continuous PPy coating on hydrophobic substrates is pointed out. We have shown, through an extensive study, that the structural, optical and electronic properties of PPy (using Ammonium persulphate as oxidant) grown on CTAB treated hydrophobic substrates are significantly different from PPy film synthesized on untreated substrates. Based on our results of surface energy analysis, we have proposed schematics to explain the role of surfactant in the growth of uniform PPy thin film.

EXPERIMENTAL

For vapor phase deposition of polypyrrole, we have selected PET (polyethylene terephthalate), ITO coated glass and silicon wafer as the substrates. The PET and ITO substrates were cleaned by ultrasonication in ethanol and DI water respectively for 30 min, while the silicon wafers were cleaned following RCA method. 0.1 M Ammonium persulphate (APS; MERCK; mixed with 100 μL of 35% hydrochloric acid was used as the oxidant. The effect of substrate modification was also studied using cupric chloride ($CuCl_2 \cdot 2H_2O$; MERCK). The first set of substrates was pretreated with cetyl trimethylammonium bromide (CTAB; LOBA; by spin coating) and then spin coated with the oxidants. We have used three different concentrations of CTAB, 0.06, 0.1, and 0.19*M*. For the second set, the oxidants were spin coated directly on the substrate surface. Polypyrrole (PPy) films were synthesized by exposing both set of oxidant coated substrates to pyrrole (SPECTROCHEM) vapor for polymerization time of 5, 10, and 20 min respectively, at 80°C in a closed environment. The PPy films were cooled to room temperature and washed repeatedly with de-ionized water and ethanol. The films have been identified in text both on the basis of the type of substrates used. Type A films indicate PPy films on CTAB pretreated substrates while Type B refer to PPy films on CTAB untreated substrates. The samples were studied using Fourier transformed infrared spectroscopy (Shimadzu FTIR-8400S), X-ray photoelectron spectroscopy (XPS) using monochromatic Al $K\alpha$ ($h\nu = 1486.6$ eV) X-ray source and a hemispherical analyzer (SPECS, HSA 3500), Atomic force microscopy (AFM; AFM-NT-MDT, Solver Pro.), field emission scanning electron microscope (FESEM Hitachi S-4800), and UV–vis spectroscopy (Shimadzu-UV-3101-PC). The field emission (FE) characteristics have been investigated in our home made high vacuum field emission setup.

The wettability or hydrophobicity of untreated PET and CTAB treated PET was studied using contact angle analysis by sessile drop method. However, instead of using image analysis algorithms, we have estimated the contact angle from the image captured digitally by a high resolution camera by using a software (NT-MDT).[29,30] The process was repeated ten to fifteen times for each drop per liquid in order to obtain the average value of the contact angles, which are reported in the text. The error in measurement of contact angle was obtained as $\pm 0.8°$.

RESULTS AND DISCUSSION

FTIR Studies

The FTIR absorption spectra of PPy films, shown in Figure 1, confirm that polypyrrole was successfully deposited using vapor phase deposition technique. Figure 1 shows the FTIR spectra in the range 500–2000 cm^{-1} for PPy films of Type A (solid line; CTAB = 0.1*M*) and Type B (dotted line) for a deposition time of 10 min. PPy films of Type A shows some well-defined features of polypyrrole. The characteristic bands around 1545 and 1430 cm^{-1} correspond to asymmetric and symmetric stretching vibration of polypyrrole ring,[31,32] while the relatively sharp peak around 1100 cm^{-1} has been identified with the stretching vibration on C–N bond.[32] Below 1000 cm^{-1}, a broad envelope with several weak signatures is observed. This broad band with several overlapping weaker bands and a maximum near 900 cm^{-1}, been associated by Davidson et al.[33] with C–H out of plane bending vibration in either quinoid or benzoid structures of pyrrole unit. C–H bending vibrations have also been identified with bands near 960 cm^{-1} by Olk et al.[34] The FTIR spectrum for Type B films, shown as dotted line in Figure 1, has a similar profile as that of Type A PPy film. However, only the bands corresponding to C–N vibration around 1100 cm^{-1} and PPy stretching vibrations at 1430 cm^{-1} can be identified clearly, due to a lower intensity of the FTIR peaks of Type B PPy films. The similar nature of the FTIR spectra suggests a semblance of Type A and Type B PPy films, since the polymerization time and other conditions were same for both the films. However, the lower intensity of the FTIR peaks of Type B films as compared to Type A may be attributed to a well-formed polypyrrole coating on CTAB treated substrates resulting in a more pronounced absorption spectra.

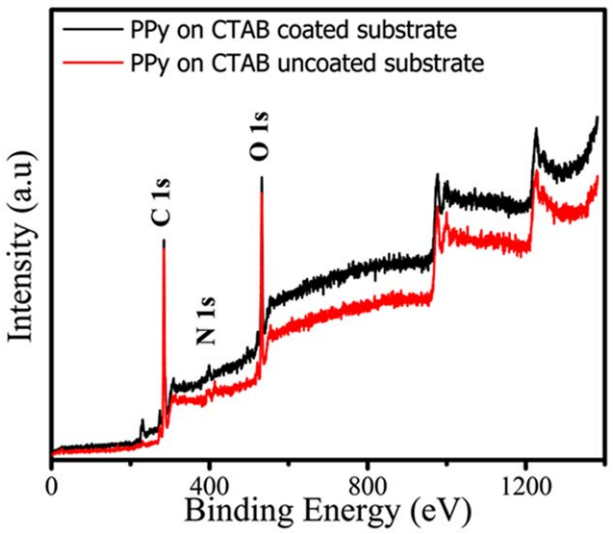

Figure 2. XPS survey scans of PPy samples on CTAB coated and uncoated hydrophobic substrates. [Color figure can be viewed in the online issue, which is available at wileyonlinelibrary.com.]

XPS Analysis

The elemental analysis of PPy on CTAB treated hydrophobic surfaces and on untreated hydrophobic substrates was performed using XPS technique. Figure 2 shows the wide survey scan XPS scan (0 to 1380 eV) of PPy thin films on CTAB coated and uncoated substrates. The presence of C, N, and O are clearly evident in XPS spectra of PPy thin films. The survey spectra match well with that reported for typical PPy samples.[35,36] However, the intensity of PPy samples on CTAB coated substrates is seen to be higher than the PPy on CTAB uncoated substrate for the entire range of spectrum scanned.

The C1*s* and N1*s* core level spectra for PPy thin films on CTAB coated substrates are shown in Figure 3(a) and (b) while the corresponding core level spectra for PPy on CTAB uncoated substrates are shown in Figure 3(c) and (d), respectively. The carbon 1*s* peak [in Figure 3(a) and (c)] is broad and asymmetric and can be fitted by two peaks, at binding energies of 284.6 and 287.9 eV. This is evident from the excellent matching between the C 1*s* spectrum and the envelope of the fitted curves. According to various literature reports, the C1*s* peak of polypyrrole is complex, containing the contribution of two superimposed lines, characteristic of the α and β carbons of the pyrrole, along with contributions at higher binding energies from other phenomena such as defectively bonded carbon atoms, steric effects, and chain termination.[37] Due to the complicated nature of this C 1*s* peak, the positions of the different fitted peaks (that are obtained on deconvolution) are not strictly defined. In general, the peaks located in the low binding energy region (283.7–284.8 eV) are assigned to α and β carbons, while the peaks at binding energy values between 285–289 eV

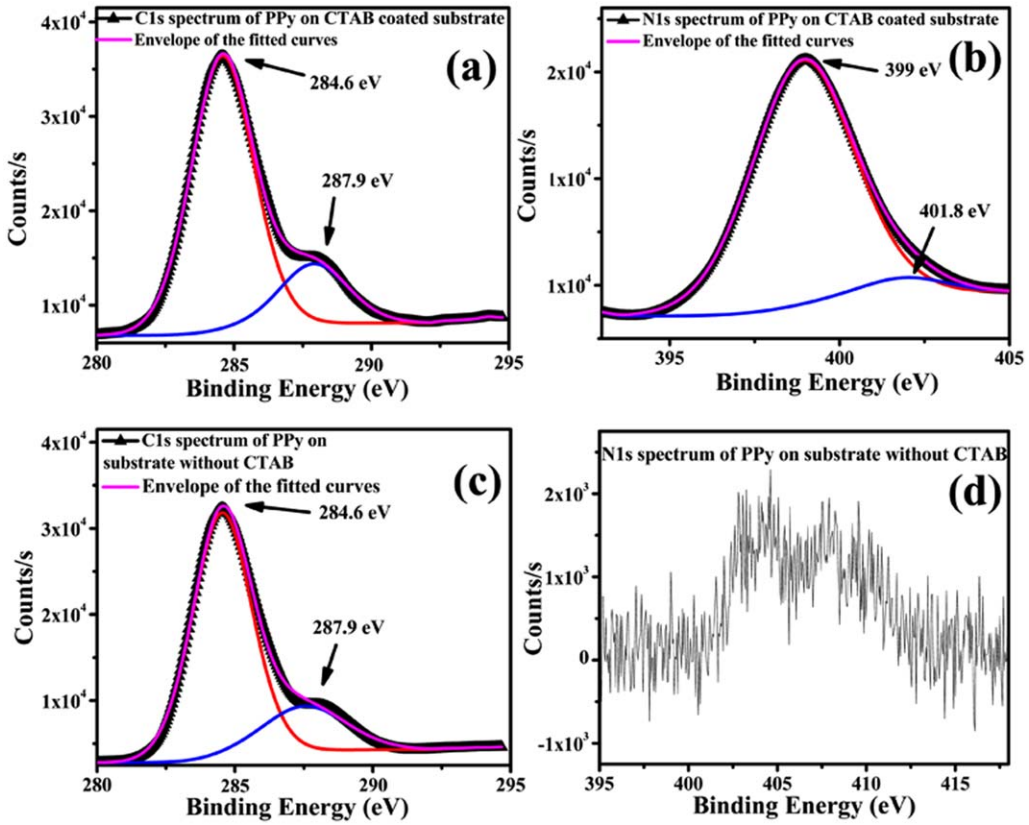

Figure 3. Core level XPS spectra of C1s and N1s of PPy on CTAB coated and uncoated hydrophobic substrates. [Color figure can be viewed in the online issue, which is available at wileyonlinelibrary.com.]

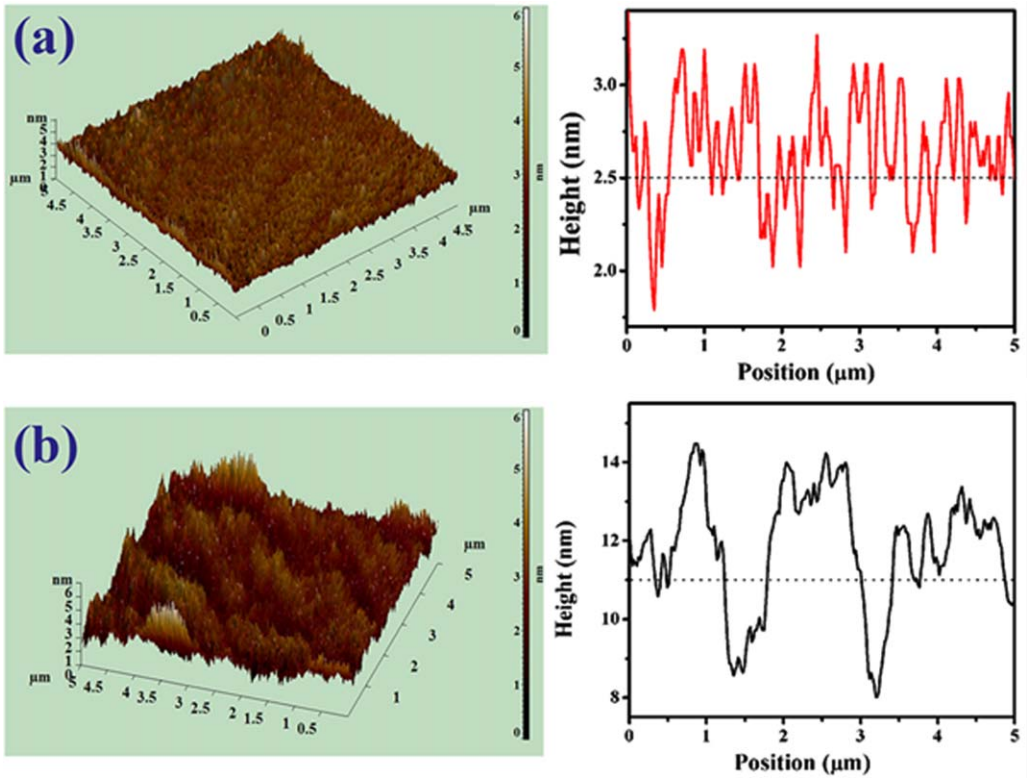

Figure 4. AFM three dimensional images and height profiles of PPy sample on (a) CTAB coated substrate and (b) CTAB uncoated substrate. [Color figure can be viewed in the online issue, which is available at wileyonlinelibrary.com.]

are assigned to carbon atoms bonded to a functional group or elements like N and O.[35–40] Figure 3(b) shows the core level spectra of the N1*s* peak of Type A PPy films. The spectrum features a major contribution at 399 eV with a shoulder at 401.8 eV. The peak around 399 eV is attributed to N atoms in the (–NH–) group of pyrrole, while the higher binding energy peak arises due to N atoms in the positively charged amine ($-NH^{+}-$) group, as a result of doping.[36,39]

In Figure 3(d), we have shown the segment of XPS spectrum where the N1*s* peak is occurs. The N1*s* peak, for Type B PPy sample, is of very low intensity so that the contribution from the background noise becomes appreciable. Moreover, the contribution of the (–NH–) group of pyrrole (at 399 eV) is also not distinguishable in Figure 3(d). The low counts per sec for the N 1*s* spectrum of Type B PPy can probably be linked to inadequate presence of PPy molecules on substrate not treated with CTAB.

The N1*s* core level spectrum plays an important role for confirming the presence of the PPy species rather than the C1*s* spectra, due to the polymeric nature of the substrate itself. The higher count of N1*s* for Type A PPy as compared to Type B PPy indicates a higher concentration of polypyrrole on the CTAB coated substrates as a result of increased adherence of PPy molecules.

Roughness Analysis Using AFM Technique

The three-dimensional representation of the surface topography of PPy samples on CTAB treated and untreated surfaces, obtained using Atomic Force Microscopy is shown in Figure 4(a) and (b), respectively.

The images were obtained by scanning an area of 5 × 5 μm. The corresponding cross sectional analysis, providing the height profile of PPy surface, as obtained by AFM, is shown alongside. The roughness of the samples, estimated by taking the average difference between five highest peaks and lowest valleys relative to the mean plane, was ~1.5 nm for Type A PPy film and ~4 nm for Type B PPy film. The smaller roughness value of PPy film on CTAB treated surface than PPy films on untreated substrates, indicating that CTAB treatment of the substrates leads to more homogeneous and smoother surfaces of the polypyrrole films. Interestingly, the average roughness of both types the PPy films reported here are much lower than that reported in literature for PPy films.[31,40]

FESEM Study

The continuity of PPy samples on both types of (untreated and treated) PET substrates, investigated using FESEM technique, for large area scan of magnification of the order of 5 μm are shown in Figure 5.

The insets show a magnified image of higher order magnification (100× k). Figure 5 (a–c) represent PPy film for untreated and treated substrate for CTAB molarity of 0.06 and 0.19*M*, respectively, for deposition time of 5 min while the PPy films deposited for 10 min for same concentration values are shown in Figure 5(d–f), respectively.

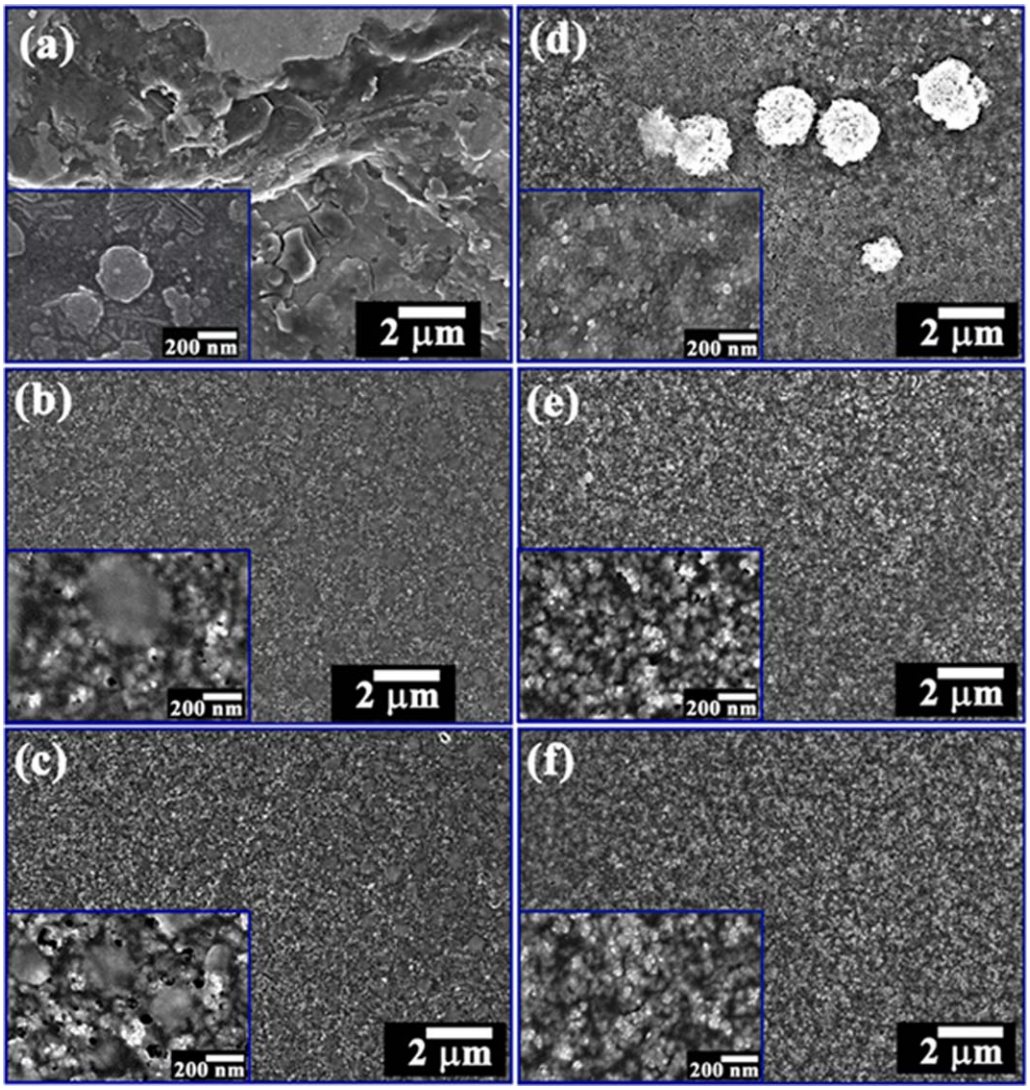

Figure 5. FESEM image of PPy films deposited from vapor phase deposition technique on (a) CTAB untreated, (b) 0.06*M* CTAB pretreated, (c) 0.19*M* CTAB pretreated PET substrates for 5 min, (d) CTAB untreated, (e) 0.06*M* CTAB pretreated, and (f) 0.19*M* CTAB pretreated PET substrates for 10 min. [Color figure can be viewed in the online issue, which is available at wileyonlinelibrary.com.]

The CTAB untreated substrates [Figure 5(a,d)] show a very non-uniform deposition of PPy film. The polypyrrole was observed only in certain isolated patches on the substrate surface with large clusters occurring in certain regions. On the other hand, when the substrates were initially treated with CTAB [Figure 5(b,c,e,f)], a definite improvement in the continuity of PPy films is observed. The uniformity of the PPy films appear to depend more on the time of polymerization than the molarity of the surfactant [as can be seen by comparing the insets of Figure 5(b) and (c) with the insets of Figure 5(e) and (f)].

The adherence and continuity of the oxidant (cupric chloride) on untreated and treated ITO coated glass substrates is shown in Figure 6 (a) and (b), respectively. $CuCl_2$ when spin coated directly on hydrophobic substrates, shows poor adherence and continuity [Figure 6(a)]. However when the same substrate is pre-coated with CTAB, a uniform oxidant layer is formed [Figure 6(b)], leading to a continuous Polypyrrole film [Figure 6(c)]. The detailed characterization of Polypyrrole (oxidized using $CuCl_2$) and difference in morphology of polymer films using different types of oxidants have been discussed in a different publication.[42]

UV–Vis Spectroscopy

Figure 7 (a) and (b) shows the UV–Vis spectra (750–300 nm) of PPy samples of Type A (CTAB = 0.19*M*) and Type B on PET substrates, for deposition time of 5 and 20 min, respectively. For comparison, we have also plotted the absorption spectra of a substrate which was prepared and treated in the same way but was not introduced in the polypyrrole deposition chamber. The absorption spectra of PPy samples is characterized by π–π^* transition which is reported to occur 400–600 nm.[31,43] However, the position of the interband transition is dependent on the level of oxidation. Bredas et al.[44] reported interband transition around 3.6 eV (~345 nm) for fully oxidized PPy film, while

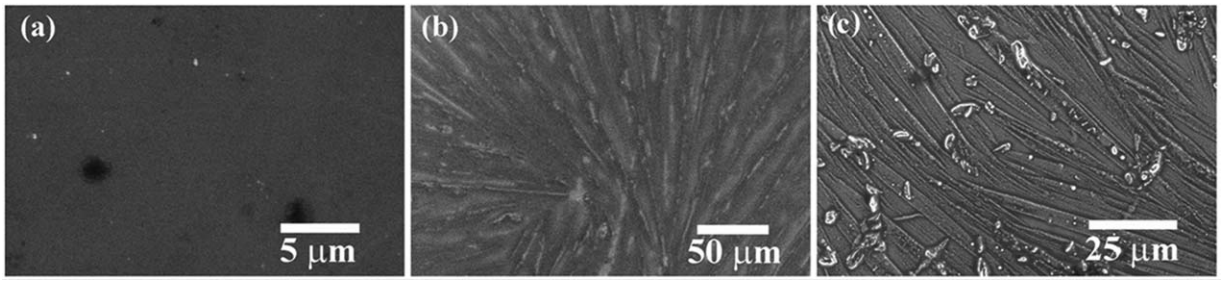

Figure 6. FESEM image of (a) $CuCl_2$ on ITO substrate, (b) $CuCl_2$ on CTAB pretreated ITO substrate, and (c) PPy on CTAB pretreated ITO substrate.

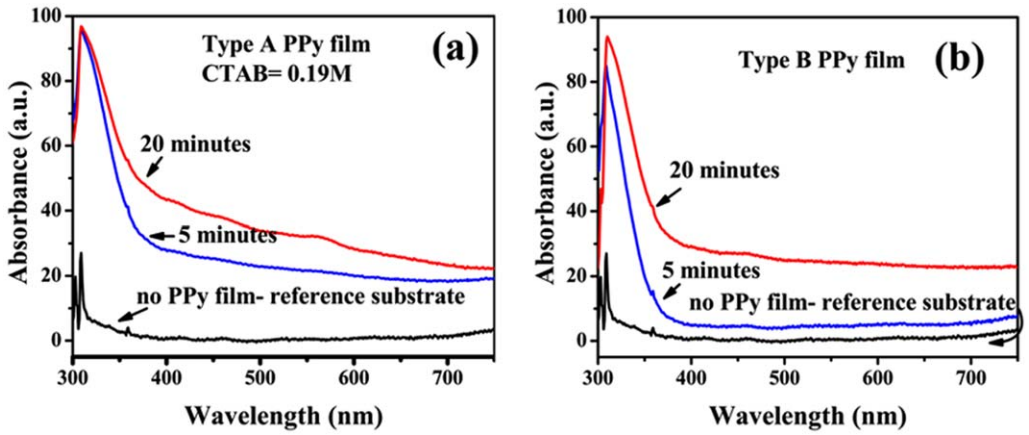

Figure 7. UV–Vis spectra of (a) Type A and (b) Type B PPy films in the range 750–300 nm. [Color figure can be viewed in the online issue, which is available at wileyonlinelibrary.com.]

Akinyeye et al.[45] reported π–π^* transition for PPyDW and PPyHCl at 291 and ~300 nm for PPyNSA sample. The amount of oxidation or doping is also responsible for appearance of additional peaks in the absorption spectra of PPy samples.

For all the samples, a strong absorption is observed around 310 nm. The absorption spectra of PPy films of Type B are similar in shape for both 5 and 20 min. The only difference that is obvious from the graph is the higher absorbance of the film deposited for 20 min as compared to the film deposited for 5 min. The effect of increase of deposition time results only in an increase of absorption, a consequence of more PPy molecules being deposited with time. The effect is however more complicated for Type A films. In this case, also, the increase in polymerization time results in higher absorbance of PPy film deposited for 20 min. However, the shape of the two curves for 5 and 20 min are not similar. While the absorbance of Type A PPy film (for 5 min) shows a strong resemblance to that of the Type B PPy films, the Type A PPy film (for 20 min) not only show absorption peak around 310 nm but also increased absorbance in the wavelength range ~350 to 600 nm, which can probably be linked to modification of the PPy structure as the interaction between the growing PPy chains increase with time.

Field Emission Studies

Figure 8 compares the typical field emission current density versus applied field (J–E) characteristics of PPy film of both Type A (solid line; CTAB = 0.1M) and Type B (dotted line) for a deposition time of 10 min. A very poor field emission characteristic is observed for Type B films. On the other hand, for the same deposition time, temperature, and molarity of the oxidant, a higher current density and lower turn on field (~3.15 V/μm) is observed for Type A films. The Fowler–Nordheim (F–N) i.e., $\ln(J/E^2)$ versus $1/E$ plot of PPy

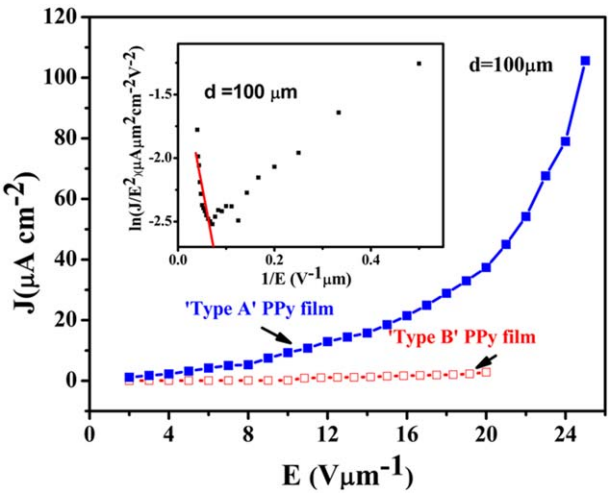

Figure 8. Field emission current density J versus Electric field E of PPy films of Type A and B deposited from vapor phase deposition technique. The inset shows the F–N plot of PPy film of Type A. [Color figure can be viewed in the online issue, which is available at wileyonlinelibrary.com.]

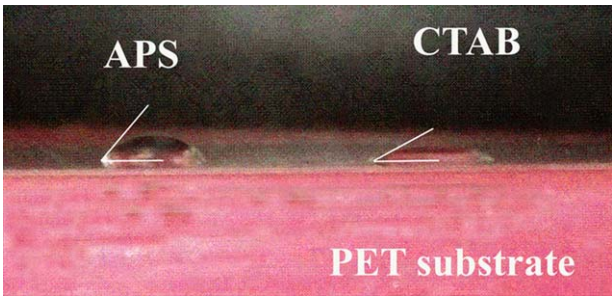

Figure 9. Drop profile image of aqueous solution of 0.1*M* APS and 0.1*M* CTAB on ultrasonically cleaned PET film. [Color figure can be viewed in the online issue, which is available at wileyonlinelibrary.com.]

films of Type A have been shown in the inset of Figure 8. The Fowler–Nordheim (F–N) model[46] can be expressed by the eq. (1)

$$J=\alpha\varphi^{-1}(\beta E)^2\exp\left[-b\varphi^{3/2}(\beta E)^{-1}\right] \quad (1)$$

where J is the emission current density, a and b are constants, ϕ is the work function (4.5 eV for PPy[47]), and β is the field enhancement factor. The enhancement factor β can be calculated from the slope of the F–N plot using eq. (2).

$$\beta=-\frac{b\varphi^{3/2}}{m} \quad (2)$$

The present calculation shows a high enhancement factor of 3234 (for Type A PPy film), which is higher than some of the reported data on polypyrrole.[48,49]

Contact Angle Analysis

Contact angle analysis offers an easy method for determining the wettability (or hydrophilicity) and adhesion of a given liquid on a solid surface. Figure 9 shows the drop profile images of aqueous solution of 0.1*M* APS and 0.1*M* CTAB, on ultrasonically cleaned PET surface. A lower contact angle ~36.7° of the CTAB solution compared to that of APS solution ~51.2° demonstrates the higher wettability of the PET surface by CTAB.

Another parameter to estimate the spreading of a liquid on a solid surface is to estimate the free surface energy. The fundamental equations that relate the interfacial tension or the free surface energy corresponding to the solid–liquid interface (γ_{SL}) to the free surface energy of the solid surface (γ_S) and liquid (γ_L) and the contact angle (θ) between the drop of liquid and the solid surface, is given by the Young's equation[50]

$$\gamma_{SL}=\gamma_S-\gamma_L\cos\theta \quad (3)$$

Each of the surface free energy components in Young's equation can be subdivided into dispersive (γ^d) and polar (γ^p) components[51]

$$\gamma_i=\gamma_D-\gamma_p \quad (4)$$

Modifying the Young's equation accordingly, Owen and Wendt obtained for a two phase (solid–liquid) system[52]

$$\gamma_{SL}=\gamma_S-\gamma_L-2\left(\gamma_S^D\gamma_L^D\right)^{0.5}=-2\left(\gamma_S^P\gamma_L^P\right)^{0.5}. \quad (5)$$

Combining eqs. (3) and (5)

$$\left(\gamma_S^D\gamma_L^D\right)^{0.5}+\left(\gamma_S^P\gamma_L^P\right)^{0.5}=0.5_{\gamma_L}(1+\cos\theta) \quad (6)$$

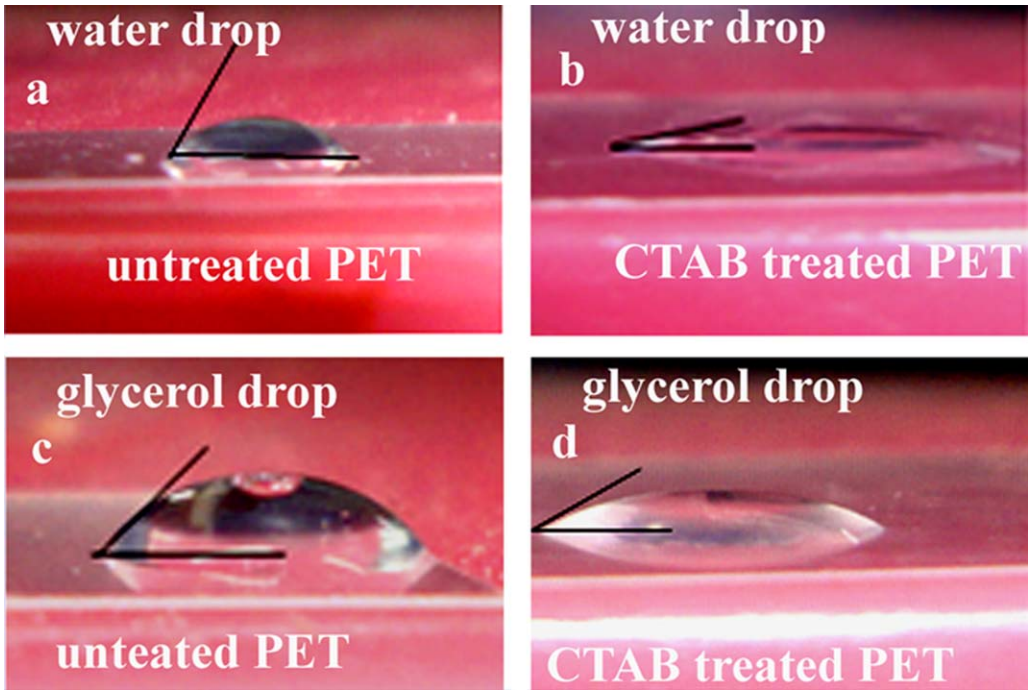

Figure 10. Drop profile image of (a) and (b) water droplet on Untreated and CTAB treated PET substrate respectively, (c) and (d) glycerol droplet on Untreated and CTAB treated PET substrate respectively. [Color figure can be viewed in the online issue, which is available at wileyonlinelibrary.com.]

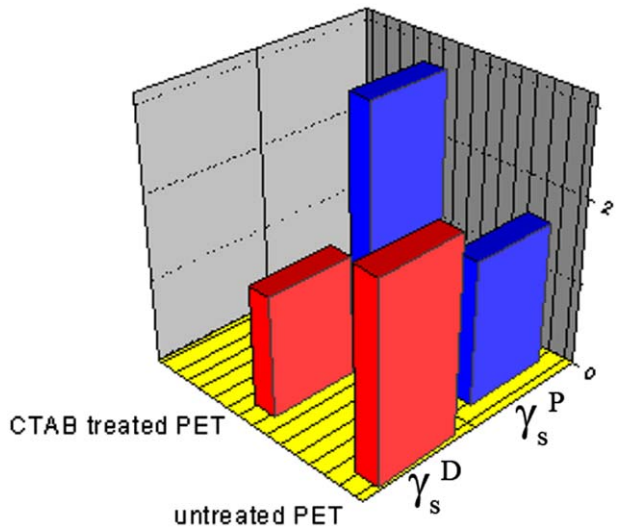

Figure 11. Variation of polar and dispersive components of surface free energy of untreated and CTAB treated PET surface. [Color figure can be viewed in the online issue, which is available at wileyonlinelibrary.com.]

We can determine the surface free energy of any given solid γ_S $(=\gamma_S^P+\gamma_S^D)$ by measuring the contact angle using two test liquids. Here, we have used water $(\gamma_L^P=51\ \mathrm{mJ/m^2}, \gamma_L^P=21.8\ \mathrm{mJ/m^2})$ and glycerol $(\gamma_L^P=30\ \mathrm{mJ/m^2}, \gamma_L^P=34\ \mathrm{mJ/m^2})$[29,30,53] as test liquids.

We have calculated the polar and the dispersive components of an untreated PET substrate and CTAB treated PET substrate using the two test liquids. As seen from Figure 10, the contact angle of the water droplet decreases from 74.5° to 19.8° and that of glycerol droplet decreases from 60.8° to 33.1° when the PET surface is treated with CTAB. The changes in the polar and the dispersive components of the surface energy for the untreated and CTAB treated surfaces are shown in Figure 11. The dispersive component (γ_S^D) of the surface free energy of the PET surface decreases from 2.33 to 1.43 $\mathrm{mJ/m^2}$ and the polar component (γ_S^P) increases from 1.71 to 2.93 $\mathrm{mJ/m^2}$ on CTAB treatment.

These results clearly indicate the surface wettability or hydrophilicity of the PET substrate increases on CTAB treatment. The adherence and continuity of PPy, film in vapor phase deposition, depends largely on the attachment of the oxidants molecules on the substrates. A necessary condition in vapor phase polymerization technique is that the substrates must first be activated with an initiator or oxidant like $FeCl_3$, $CuCl_2$, etc.[54] Since polypyrrole is formed wherever the monomer vapors interact with the oxidant molecule, it is mandatory that both the oxidant and polymer should adhere to the substrate for formation of uniform and stable PPy film. Hydrophilic oxidants like APS and $CuCl_2$ on the other hand spread non-uniformly, due to their poor attachment on the hydrophobic substrates, forming lumps or clusters in certain regions, resulting in PPy films that have a scattered, uneven morphology.

The reason behind uniformity of PPy films on CTAB treated substrates can be attributed to the structure of CTAB itself. CTAB molecule consists of a hydrophobic tail with a hydrophilic head group. Due to this structure, CTAB spreads readily on both hydrophobic and hydrophilic substrates. Pre-coating the hydrophobic substrates with CTAB increases the hydrophilicity or wettability as seen from the surface free energy values. This ensures a more uniform spreading of the aqueous solution of the oxidant. Since the pyrrole vapors polymerize directly at the oxidant adsorbed sites, a uniform oxidant layer ensures a continuous and denser PPy film deposition than on an untreated substrate. Introduction of polar groups on hydrophobic substrates by means of a surfactant coating, also promotes different types of interactions like dipolar interactions, van der Waals forces or hydrogen bonds between the polymer coating

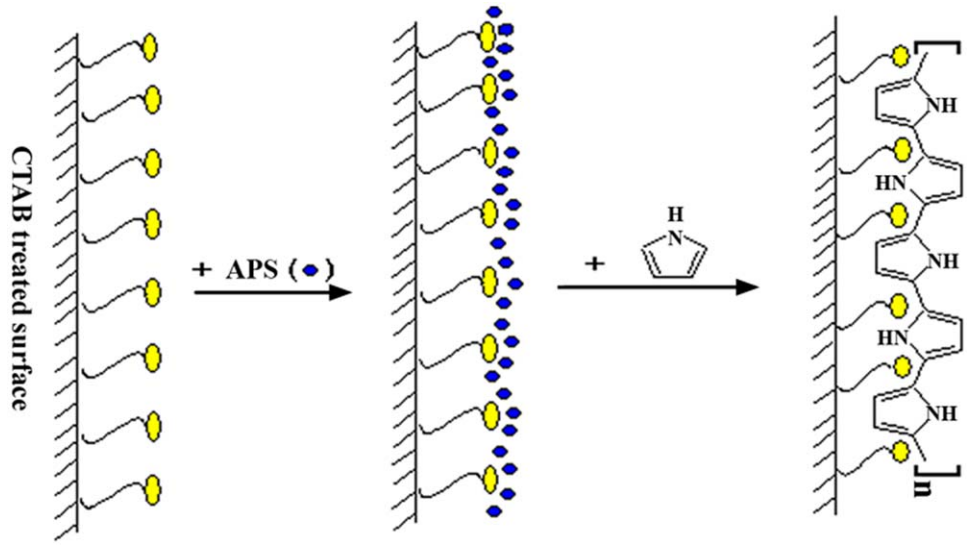

Figure 12. Schematics of PPy deposition from vapor phase on CTAB treated surface. [Color figure can be viewed in the online issue, which is available at wileyonlinelibrary.com.]

and the substrate surface, so that the polymer films are not swept away when the polymer films are repeatedly washed after polymerization. The schematics of PPy deposition on CTAB treated surface is shown in Figure 12.

CONCLUSIONS

CTAB has been widely used as micelle formation agent in the synthesis of nanostructured PPy. However, these surfactants can find an alternate application as an adhering agent in vapor phase deposition of PPy, especially on hydrophobic surfaces. As seen in this study, oxidants like APS and $CuCl_2$ do not spread easily on hydrophobic substrates. However, when treated with CTAB, the same substrates show a lower contact angle for adherence of hydrophilic liquids. Subsequent polymerization of pyrrole from vapor phase on these substrates result in PPy films with higher absorption in infrared and visible regions, a lower surface roughness, a more uniform morphology and higher field emission currents than PPy films on CTAB untreated substrates, under the same polymerization conditions. We propose that coating substrates with CTAB, prior to polymerization, improves their hydrophilicity and hence promotes the adhesion of the oxidant ($APS/CuCl_2$) resulting in deposition of uniform PPy film.

ACKNOWLEDGMENTS

One of the authors (N. Dutta Gupta) wishes to thank the University Grants Commission (UGC), the Government of India, for awarding her Dr. D. S. Kothari postdoctoral fellowship during the execution of the work. The authors also wish to acknowledge the UGC for "University with potential for excellence (UPEII)" scheme.

REFERENCES

1. Wesling, B.; Posdorfer, J. *J. Electrochim. Acta* **1999**, *44*, 2139.
2. Guiseppi-Elie, A.; Wilson, A. M.; Tour, J. M.; Brakmann, T. W.; Zhang, P.; Allera, D. L. *Langmuir* **1995**, *11*, 1768.
3. Hakansson, E.; Amiet, A.; Nahavandi, S.; Kaynak, A. *Eur. Polym. J.* **2007**, *43*, 205.
4. Duchet, J.; Legras, R.; Demoustier-Champagne, S. *Synth. Met.* **1998**, *98*, 113.
5. Orinakov, R.; Kupkova, M.; Orinak, A.; Fedorkova, A.; Dudrov, E. *Surf. Interface Anal.* **2010**, *42*, 1706.
6. West, R.; Zeng, X. *Langmuir* **2008**, *24*, 11076.
7. Cheing, K. M.; Bloor, D.; Stevens, G. L. *Polymer* **1988**, *29*, 1709.
8. Diaz, A. F.; Rubinson, J. F.; Mark, H. B. *Adv. Polym. Sci* **1988**, *84*, 113.
9. Keneko, M.; Wohrle, D. *Adv. Polym. Sci.* **1988**, *84*, 141.
10. Khedkar, S. P.; Radhakrishnan, S. *Thin Solid Films* **1997**, *303*, 167.
11. Qi, Z. G.; Rees, N. G.; Pickup, P. G. *Chem. Mater.* **1996**, *8*, 701.
12. Kuhn, H. H.; Child, A. D. In Handbook of Conducting Polymers; Skotheim, T. A., Elsenbaumer, R. L., Reynolds, J. R., Eds.; Marcel Dekker: New York, **1998**; Chapter *19*, p 993.
13. Willcut, R. J.; McMarthy, R. L. *J. Am. Chem. Soc.* **1994**, *116*, 10823.
14. Sayre, L. N.; Collard, D. M. *Langmuir* **1997**, *13*, 714.
15. Radhakrishnan, S.; Saini, D. R. *Synth. Met.* **1993**, *58*, 243.
16. Radhakrishnan, S.; Khedkar, S. P. *Synth. Met.* **1996**, *79*, 219.
17. Simon, A.; Ricco, A. J.; Wrighton, M. J. *J. Am. Chem. Soc.* **1982**, *104*, 2031.
18. Wu, C. G.; Chen, C. Y. *J. Mater. Chem.* **1997**, *7*, 309.
19. Cossement, D.; Plumier, F.; Delhale, J.; Havesi, L.; Mekhalif, Z. *Synth. Met.* **2003**, *138*, 529.
20. Faverolle, F.; Attias, A. J.; Bloch, B.; Audebert, P.; Andrieux, C. P. *Chem. Mater.* **1998**, *10*, 740.
21. Cai, X.; Jaehne, E.; Adler, H. J.; Guo, W. *Chin. J. Chem.* **2010**, *28*, 1272.
22. Intelmann, C. M.; Rammelt, U.; Plieth, W.; Cai, X.; Jahne, E.; Adler, H. P. *J. Solid State Electrochem.* **2006**, *11*, 1.
23. Molina, J.; Oliveira F. R.; Souto, A. P.; Esteves, M. F.; Bonastre, J.; Cases, F. *J. Appl. Polym.* **2013**, *129*, 422.
24. Oh, K. W.; Kim, S. H.; Kim, E. A. *J. Appl. Polym. Sci.* **2001**, *81*, 684.
25. Garg, S.; Hurren, C.; Kaynak, A. *Synth. Met.* **2007**, *157*, 41.
26. Sevil, B.; Zuhal, K. *Macromol. Symp.* **2010**, *295*, 59.
27. Zhang, X.; Zhang, J.; Song, W.; Liu, Z. *J. Phys. Chem. B* **2006**, *110*, 1158.
28. Dai, T.; Yang, X.; Lu, Y. *Nanotechnology* **2006**, *17*, 3028.
29. Banerjee, D.; Mukherjee, S.; Chattopadhyay, K. K. *Carbon* **2010**, *48*, 1025.
30. Yang, M. W.; Lin, S. Y. *Colloids Surf. A Physicochem. Eng. Aspects* **2003**, *220*, 199.
31. Reung-U-Rai, A.; Prom-Jun, A.; Prissanaroon-Ouajai, W.; Ouajai, S. *J. Met. Mater. Mine.* **2008**, *18*, 27.
32. Wei, M.; Dai, T.; Lu, Y. *Synth. Met.* **2010**, *160*, 849.
33. Davidson, R. G.; Turner, T. G. *Synth. Met.* **1995**, *72*, 121.
34. Olk, C. H.; Beetz, C. P. Jr.; Heremans, J. *J. Mater. Res.* **1988**, *3*, 984.
35. Jaramillo, A.; Lisa D. Spurlock, L. S.; Young, V.; Brajter-Toth, A. *Analyst* **1999**, *124*, 1215.
36. Idla, K.; Talo, A.; Niemi, H. E.-M.; Forse, O.; Yläsaari, S. *Surf. Interface Anal.* **1997**, *25*, 837.
37. Atanasoska, L.; Naoi, K.; Smyrl, W. H. *Chem. Mater.* **1992**, *4*, 988.
38. Street, G. B.; Clarke, T. C.; Geiss, R. H.; Lee, V. Y.; Nazzal, A.; Pfluger, P.; Scott, J. C. *J. Phys. I* **1983**, *C3*, 599.
39. Pigois-Landureau, E.; Nicolau, Y. F.; Delamar, M. *Synth. Met.* **1995**, *72*, 111.
40. Dejeu, J.; Taouil, A. E.; Rougeot, P.; Lakard, S.; Lallemand, F.; Lakard, B. *Synth. Met.* **2010**, *160*, 2540.
41. Adhikari, A.; Radhakrishnan, S.; Vijayan, M. *J. Appl. Polym. Sci.* **2012**, *125*, 1875.
42. Dutta Gupta N.; Das S.; Chattopadhyay K. K. (to be Communicated).
43. Gretha, S.; Trivedi, D. C. *Mater. Chem. Phys.* **2004**, *88*, 388.

44. Bredas, J. L.; Scott, J. C.; Yakushi, K.; Street, G. B. *Phys. Rev. B* **1984**, *30*, 1023.

45. Akinyeye, R.; Michira, I.; Sekota, M.; Al-Ahmed, A.; Baker, P.; Iwuoha, E. *Electroanalysis* **2006**, *18*, 2441.

46. Fowler, R. H.; Nordheim, L. *Proc. R. Soc. London A* **1928**, *119*, 173.

47. Joo, J.; Lee, S. J.; Park, D. H.; Lee, J. Y.; Lee, T. J.; Seo, S. H.; Lee, C. J. *Electrochem. Solid-State Lett.* **2005**, *8*, H39.

48. Joo, J.; Kim, B. H.; Park, D. H.; Kim, H. S.; Seo, D. S.; Shim, J. H.; Lee, S. J.; Ryu, K. S.; Kim, K.; Jin, J. I.; Lee, T. J.; Lee, C. *J. Synth. Met.* **2005**, *153*, 313.

49. Kim, B. H.; Park, D. H.; Joo, J.; Yu, S. G.; Lee, S. H. *Synth. Met.* **2005**, *150*, 279.

50. Young, T. *Phil. Trans. R Soc. Lond.* **1805**, *95*, 65.

51. Żenkiewicz, M. *J. Achiev. Mater. Manuf. Eng.* **2007**, *4*, 137.

52. Owens, D. K.; Wendt, R. C. *J. Appl. Polym. Sci.* **1969**, *13*, 1741.

53. Ostrovskaya, L.; Podesta, A.; Milani, P.; Ralchenko, V. *Eur. Phys. Lett.* **2003**, *63*, 401.

54. Kim, J.; Sohn, D.; Sung, Y.; Kim, E. R. *Synth. Met.* **2003**, *132*, 309.